

Adapter-Enhanced Semantic Prompting for Continual Learning

Baocai Yin¹ Ji Zhao¹ Huajie Jiang^{1†} Ningning Hou² Yongli Hu¹
Amin Beheshti² Ming-Hsuan Yang³ Yuankai Qi²

¹School of Information Science and Technology, Beijing University of Technology, China

²School of Computing, Macquarie University, Australia

³Electrical Engineering and Computer Science, University of California at Merced, USA

Abstract

Continual learning (CL) enables models to adapt to evolving data streams. A major challenge of continual learning is catastrophic forgetting, where new knowledge overwrites previously acquired knowledge. Prompt-based CL methods receive increasing attention due to the avoidance of computing-heavy replay of old data. In this paper, we introduce a new lightweight framework for continual learning called Adapter-Enhanced Semantic Prompting (AESP). It stands out from the existing prompt-based CL framework in three aspects. First, we propose to utilize a (semantic prompt, learnable visual prompt) pair to represent task-specific knowledge instead of just visual prompts as in existing works. The semantic prompt is a representative summary of each task, obtained via a large language model, e.g., BERT, using class labels as input. It provides extra rich information to visual prompts. Second, the semantic prompt is also used as input for our Adapter-enhanced ViT. Both the newly introduced semantic prompt and adapters enable better adaptation of frozen ViTs for new tasks. Third, we design a strong Query-Key matching method for selecting an appropriate task prompt pair to improve final prediction accuracy. Extensive experiments across three continual learning datasets demonstrate that the proposed framework achieves favorable performance compared to several state-of-the-art approaches.

1. Introduction

Continual learning (CL) [2, 4, 25, 46, 47, 56] aims to enable models to continuously learn from evolving data streams and adapt to new environments. Different from traditional machine learning models [21, 30] that are trained on fixed datasets and become static after training, CL enables mod-

els to accumulate existing knowledge and learn new information with new-task data and existing models, which avoids retaining all old task data and retrain the model [15, 25]. CL has received increasing attention in recent years due to its promising capability to deal with challenges like data privacy and memory resource limitations [29, 34, 39].

However, CL suffers from catastrophic forgetting [13, 31, 41], which is caused by the overwriting of old knowledge when learning new tasks, resulting in a significant decline in performance for previous tasks. To address this issue, some approaches [3, 19, 45] propose to retain a few representative samples from the old tasks for knowledge replay. When the next task comes, the retained samples are replayed with the new task data. Such approaches have demonstrated their effectiveness in mitigating the model’s forgetting. However, retaining samples may impose a memory burden and introduce privacy leakage risks. Besides retaining samples, [5, 25] propose to add new branches to the network for each new task, which increases the model size and results in slower inference speed and lower efficiency.

In recent years, prompt-based methods [23, 35, 44, 48, 49] have been proposed for CL thanks to their ability to leverage the knowledge of pre-trained Visual Transformer (ViT) with fewer parameters and higher efficiency. As is shown in Figure 1 (a), these methods learn visual prompts to efficiently adapt the pre-trained ViT model to the CL tasks. However, they rely solely on visual information, which may cause the model to struggle in acquiring knowledge with strong generalization capabilities, especially when the training data is limited and lacks sufficient diversity. By contrast, class semantic information extracted by large language models is more generalized and adaptable across tasks. Models like BERT [10] and CLIP [38] align samples of the same class with the corresponding semantic information associated with their class label, thus creating a more generalized feature space. This alignment enables the model to maintain robustness when encountering unseen

[†]Corresponding authors

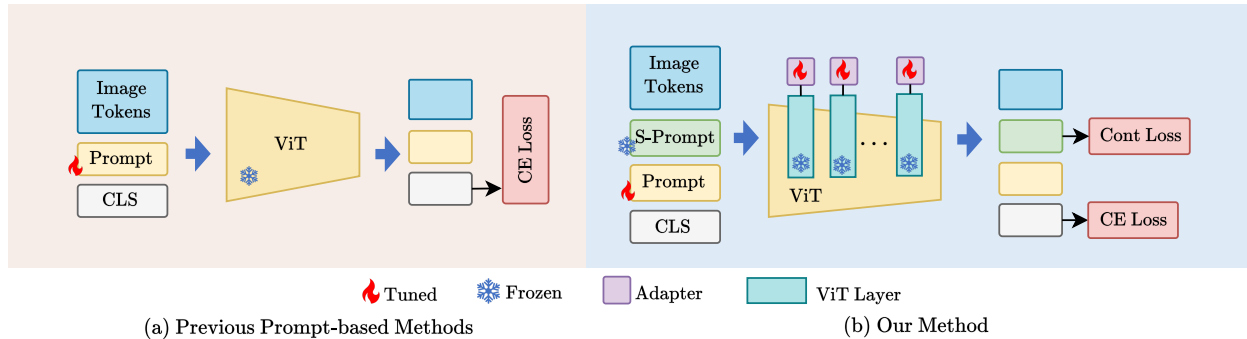


Figure 1. Comparison between previous prompt-based approaches and our framework. Previous approaches mainly use visual prompts to update the image features. In contrast, our method introduces semantic prompts (S-Prompts) to enrich the semantic information and embeds a fine-tunable adapter structure to effectively learn adaptive image features.

samples of the same class, as the model learns to focus on the shared semantic features, rather than relying solely on specific visual features.

In this work, we propose a novel Adapter-Enhanced Semantic Prompting (AESP) framework, which introduces semantic information to enhance the generalization of the pre-trained ViT model for more adaptive visual feature learning. However, semantic and visual information differ significantly in terms of representation and feature space. Relying solely on the attention modules in a pre-trained ViT may not effectively fuse these two types of information. To address this, we introduce small, learnable adapter modules into the ViT model. As shown in Figure 1 (b), adapters are integrated into each layer of the ViT to help the model better accommodate semantic information and facilitate the effective interaction between visual and semantic features. Therefore, the model not only combines multimodal features more effectively but also enables the learned knowledge to exhibit better generalization ability, leading to improved adaptability in the new coming tasks.

To accurately select the task-specific prompt for feature adaptation, we propose a new prompt-key matching method that combines four matching strategies to ensure that the most relevant prompts are selected from the prompt pool. Extensive experiments demonstrate that our proposed AESP framework can effectively improve the model’s performance across various incremental tasks.

The main contributions are summarized as follows:

- We propose a novel Adapter-Enhanced Semantic Prompting framework for continual learning, which integrates multimodality prompts and adapters to facilitate adaptive feature learning.
- We propose to utilize semantic prompts to improve the generalization ability of visual features and design a cosine contrast loss for effective optimization.
- We integrate multiple prompt-key matching strategies to improve the accuracy of prompt selection.

- Extensive experiments on three continual learning datasets demonstrate that our method achieves favorable performance compared to several state-of-the-art approaches.

2. Related Work

Continual Learning. Continual Learning (CL) is an advanced area within machine learning that allows models to continuously learn new information while preserving previously acquired knowledge [4, 25, 47, 54, 56]. However, the process of acquiring new knowledge can overwrite earlier learning, leading to the issue of catastrophic forgetting [13, 31, 41]. To address this, CL techniques implement various strategies to balance retaining old knowledge and integrating new information. One such approach involves regularization methods, which safeguard critical parameters by imposing constraints that prevent significant changes that might erase previously learned knowledge [1, 33, 50]. Another approach called knowledge distillation, is frequently used to facilitate a smooth transition between older and newer models [11, 26, 27]. Parameter isolation strategies [40, 51, 53] protect existing knowledge by freezing certain parameters tied to earlier tasks and allocating new parameters for incoming tasks. However, this can lead to increased model complexity and maintenance overhead. Rehearsal methods [3, 6, 14] strengthen previous learning by revisiting examples from earlier tasks. While effective, these methods require additional memory and may pose data privacy concerns. These challenges drive the pursuit of innovative rehearsal-free approaches to manage better catastrophic forgetting in continual learning systems.

Prompt-based Method. The above-mentioned methods require training a model from scratch, whereas recent developments in continual learning focus on fine-tuning from pre-trained networks [8, 28, 36, 37]. This strategy is gaining attention due to its enhanced adaptability and learning efficiency. A common fine-tuning approach is

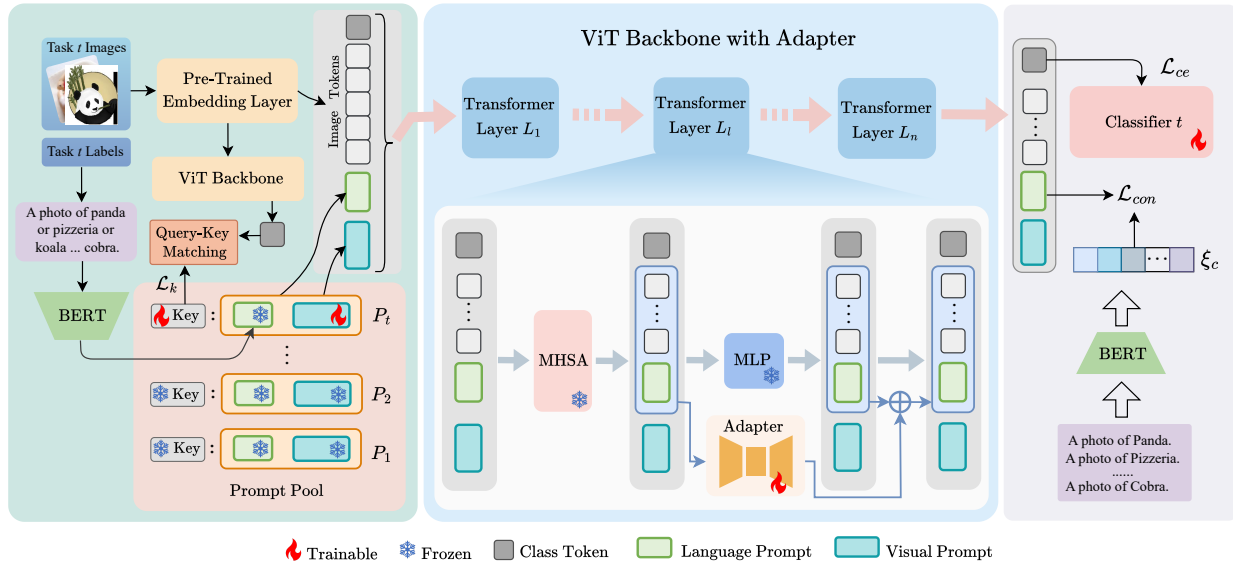


Figure 2. Main architecture of our method. Our model incorporates visual prompts and semantic prompts generated by a large language model to enrich the input information (Section 3.3). An integrated Query-Key matching mechanism is introduced to select the relevant prompts (Section 3.4). The selected prompts alongside the image tokens are then fed into a novel backbone network, which includes adapters that can adapt to varying depths of the backbone network for feature refinement and learning (Section 3.5). The final output features are optimized using classification loss and the proposed cosine contrastive loss to guide the model’s fitting process (Section 3.6).

prompt-based fine-tuning. Prompt-based approaches like L2P [49] and DualPrompt [48] innovate by using learnable prompts to dynamically guide the model’s focus during training and inference phases. These prompts serve as modular instructions inserted into models, ensuring that the acquired knowledge is encapsulated and readily retrievable, thus maintaining performance across a variety of tasks. The integration of key-query mechanisms, as seen in methods like CODAPrompt [42], further refines this process by allowing more nuanced, context-sensitive prompt applications, significantly expanding the model’s ability to handle diverse learning scenarios without overwriting existing knowledge. However, the model’s predictions can be adversely affected when irrelevant prompts are selected during inference. CPrompt [16] proposes a consistent prompting approach to improve the robustness of prompts, minimizing this interference as much as possible.

Adapter-based Method. Adapter architectures [9, 20] were first proposed for fine-tuning LLMs, performing task adaptation by introducing a small amount of additional learnable parameters while allowing the parameters of the backbone network to remain fixed. Thus this method achieves a high degree of parameter sharing. Leveraging these strengths, SSIAT [43] integrates adapters into the continual learning field, employing a prototype shift strategy to combat the model forgetting problem that arises from adapter parameter updates. This has led to the efficient fine-tuning of pre-trained networks and has resulted in superior

performance compared to prompt-based approaches. The C-ADA [15] employs an expandable strategy for adapter parameters and utilizes regularization techniques to guide the direction of parameter updates. This could mitigate the interference between new and old knowledge. EASE [55] offers another idea, designing a distinct lightweight adapter module for each new task and utilizing a semantic-guided prototype complement strategy to synthesize new features for old classes. The aforementioned adapter-based methods have demonstrated good performance in reducing catastrophic forgetting.

Different from previous approaches, we propose using a semantic prompt to improve the generalization ability of image features and design adapters to effectively fuse semantic information with vision information, thereby enabling the features more adaptive to the continual learning tasks.

3. Methodology

3.1. Overview

In response to the challenges posed by continual learning, we propose a novel Adapter-Enhanced Semantic Prompting framework (AESP). As illustrated in Figure 2, our framework incorporates two types of prompts: randomly initialized visual prompts and semantic prompts generated by a text encoder. Since each task requires specific prompts, selecting the most relevant task-specific prompts is crucial for effective learning. To address this, we introduce a novel

integrated Query-Key matching mechanism, which combines multiple matching strategies to significantly improve the precision of prompt selection.

Once the relevant prompts are selected, they are added to the input of the network. Given that visual and semantic features differ significantly in terms of their representations and feature spaces, we integrate adapters into each layer of the ViT network via residual connections to effectively fuse these two modalities. As a result, the final output features of the model contain both visual and semantic information. To enable the model to learn generalized knowledge from the semantic prompts, we design a novel cosine contrast loss function that enforces the alignment of the semantic prompts within a specific class semantic space.

3.2. Preliminary

Class-Incremental Learning Formulation. Continual learning aims to enable models to learn from changing data across sequential tasks while retaining knowledge from previous task data. For a dataset \mathcal{D} with N_c distinct classes $\mathcal{D} = \{\mathcal{D}_1, \dots, \mathcal{D}_{\mathcal{T}}\}$, where $\mathcal{T} = N_c/N_{inc}$ represents the number of incremental tasks, and N_{inc} is the number of classes to be trained in each incremental task stage. The dataset for t -th task is denoted as $\mathcal{D}_t = \{(x_i^t, y_i^t)\}_{i=1}^{N_t}$, where N_t is the number of samples, and x_i^t is the i -th image and y_i^t is the label of x_i^t in the t -th task; $y_i \in Y(t)$, where $Y(t)$ represents the class set in task t . After the t -th session, all the classes learned are denoted as $\mathcal{Y} = Y(1) \cup Y(2) \cup \dots \cup Y(t)$. The objective of this framework is to train a mapping function capable of predicting the class of an input image x for all trained classes $\in \mathcal{Y}$. The datasets are fed to models one by one to mimic data stream. In this work, we focus on Class-Incremental Learning (CIL) [14, 32, 56], where the task boundaries are explicit, but the task identity is unknown during testing.

Pre-trained Visual Transformer Backbone. The backbone of our network is a pre-trained visual Transformer (ViT) [12] on the ImageNet dataset. This backbone consists of an embedding layer f_e , and several Multi-Head Self-Attention (MHSA) blocks f_b where $b = 1, 2, \dots, N_b$. Given an input image $x \in \mathbb{R}^{H \times W \times C}$ from \mathcal{D}_t , the image is first processed by the embedding layer into a sequence of features written in the form of matrix $\xi_e = f_e(x) \in \mathbb{R}^{L_{img} \times d}$, where L_{img} is the number of tokens, and d is the embedding dimension. Then, a class token $[CLS] \in \mathbb{R}^d$ is prepended to the features ξ_e , and they are fed into MHSA blocks to get the final representation $\xi_{cls} \in \mathbb{R}^d$ for the image. ξ_{cls} is used to train a task-specific classifier $\Phi(\cdot; \phi)$, where $\phi = \{\phi_1, \phi_2, \dots, \phi_{\mathcal{T}}\}$ denotes the parameters of each classifier.

3.3. Semantic and Visual Prompt

We use semantic prompts to enhance the generalization ability of visual features. Specifically, we form a seman-

tic description R_{lan} as:

$$\text{“A photo of \{class1\} or \{class2\} \dots or \{classN_{inc}\}.”} \quad (1)$$

for the t -th task dataset comprising the class names. Here, $class1, class2, \dots, classN_{inc}$ will be replaced with the class names from $\mathcal{Y}(t)$. We then employ the pre-trained large language model BERT [10] as a semantic feature extractor to transform R_{lan} into a text embedding:

$$P_s = \text{BERT}(R_{lan}), \quad (2)$$

where $P_s \in \mathbb{R}^d$ represents the task-level semantic prompt.

Like existing works, we also employ trainable visual prompts to extract classification knowledge from the visual feature space. We define the visual prompt as $P_v \in \mathbb{R}^{L_{vp} \times d}$, where L_{vp} is the length of the visual prompt. P_v is randomly initialized at the start of training. These visual prompts are trained during each incremental session, and all trained prompts will be stored in a prompt pool.

Then, the input of the ViT backbone network consist of multiple parts as

$$\hat{x} = [\xi_{cls}, \xi_e, P_s, P_v]. \quad (3)$$

where ξ_{cls} is a class token, ξ_e refers to the image tokens, P_s and P_v denote the semantic prompt and visual prompt, respectively. We define $\hat{x} \in \mathbb{R}^{L_{\hat{x}} \times d}$ to represent the input information for the ViT backbone network, and $L_{\hat{x}} = 1 + L_{img} + 1 + L_{vp}$ as the total number of input token lengths.

3.4. Integrated Query-Key Matching Mechanism

Previous prompt-based methods typically train a separate prompt for each task and use a Query-Key matching mechanism to select an appropriate task prompt for image classification, where the query feature is derived from the input image and the key is a learnable vector associated with the prompt.

However, the query features of different classes within the same task can vary significantly, which hinders selecting an appropriate task prompt. To address this problem, [16] introduced a Multi-Key mechanism, where each class within a task is assigned a unique key. The Multi-Key mechanism focuses on matching the query feature with the key of each individual class. Despite improvement, achieving accurate matching at the early stages of model training remains challenging. To further enhance prompt selection accuracy, we propose a new method called the Integrated Query-Key Matching Mechanism.

Our method is built upon the multi-key matching mechanism, where the trainable keys are denoted as $\mathcal{K} = \{\mathcal{K}_1, \mathcal{K}_2, \dots, \mathcal{K}_t, \dots, \mathcal{K}_{\mathcal{T}}\}$. There are N_{inc} keys for each key set $\mathcal{K}_t = \{K_i^t\}_{i=1}^{N_{inc}}$, where $K_i^t \in \mathbb{R}^d$ represents

the key of the i -th class in t -th task. When training begins, the query image is fed into the frozen ViT to extract query feature $q \in \mathbb{R}^d$. Then, we calculate the cosine similarity between query feature q and all keys in the current training task, resulting in a score vector $\hat{\ell} = [\cos(q, K_1^t), \cos(q, K_2^t), \dots, \cos(q, K_{N_{inc}}^t)]$. We further convert the score vector into a probability distribution via softmax:

$$\ell_c = \frac{e^{\hat{\ell}_c}}{\sum_{j=1}^{N_{inc}} e^{\hat{\ell}_j}}, \quad (4)$$

where $c \in \{1 : N_{inc}\}$, and ℓ_c is the similarity score of the c -th key after softmax. To encourage the query feature close to its key and far away from other keys, we use the cross-entropy loss function [52] as the multi-key loss:

$$\mathcal{L}_k = -\frac{1}{N_{inc}} \sum_i^{N_{inc}} y_i \log(\ell), \quad (5)$$

where y_i is the ground truth label for the input image x_i .

Despite success, we observe that this multi-key mechanism may select incorrect prompts when classes in other tasks are similar to those in the current task, finally leading to wrong image classification. To address this issue, we introduce an extra measurement based on entropy, which reflects decision confidence:

$$H(\ell) = -\sum_{i=1}^{N_{inc}} \ell_i \log(\ell_i). \quad (6)$$

Additionally, to further enhance the accuracy of the selection prompts, we calculate the feature mean of each query class as prototype $\xi_q \in \mathbb{R}^D$. Then, the similarity between the query features and all prototypes for the t -th task is calculated and processed using the softmax function. Consequently, we obtain a new probability distribution vector as output:

$$\zeta_c = \frac{e^{\cos(q, \xi_{q,c})}}{\sum_{j=1}^{N_{inc}} e^{\cos(q, \xi_{q,j})}}, \quad (7)$$

where $c \in \{1 : N_{inc}\}$ is the index of each class. Similarly, its entropy is used to improve query-key matching:

$$H(\zeta) = -\sum_{i=1}^{N_{inc}} \zeta_i \log(\zeta_i). \quad (8)$$

During the inference process, the model integrates four strategies to select prompts, where each strategy is formu-

lated as:

$$P_1 = \arg \max_{t \in T} \{\ell_t\}, \quad (9)$$

$$P_2 = \arg \min_{t \in T} \{H(\ell_t)\}, \quad (10)$$

$$P_3 = \arg \max_{t \in T} \{\zeta_t\}, \quad (11)$$

$$P_4 = \arg \min_{t \in T} \{H(\zeta_t)\}, \quad (12)$$

$T \in \{1 : \mathcal{T}\}$ represents the number of tasks already trained. Then, we adopt a voting strategy [7] to select the final task prompt. If all outputs differ, the P_1 is chosen by default as the final prediction result. The model uses the predicted task prompt to carry out the remaining computation.

3.5. Transformer Layers with Adapter

Previous prompt-based methods [48, 49] primarily focus on the input and output of pre-trained models, overlooking the internal learning processes and feature extraction. This limits the model’s generalization capability, making it difficult to adapt to new data. To address this problem, we propose incorporating adapter structures within the layers of pre-trained models.

An adapter typically consists of a down-projection matrix $W_{down} \in \mathbb{R}^{d \times d'}$, a non-linear activation function such as ReLU, and an up-projection matrix $W_{up} \in \mathbb{R}^{d' \times d}$. Here, d' refers to the input dimension of the ReLU activation layer. Let x_{in} denote the input to the adapter. An adapter can be formalized as:

$$x_{out} = W_{up,L}(\text{ReLU}(W_{down,L} \cdot x_{in})), \quad (13)$$

$$x_{in} = [\xi_e, P_s], \quad (14)$$

where L represents the L -th layer of the backbone. To enable using semantic information to guide the model in learning more generalized visual features, we input the image token ξ_e and P_s into the adapter. As training, the parameters within the adapter retain knowledge learned from the data.

Thanks to our new Query-Key matching mechanism proposed in Section 3.4, which significantly enhances task-matching accuracy. We adopt task-specific adapter parameters to address the forgetting problem caused by the updating of adapter parameters. When a new task comes, the adapter will train new parameters while retaining the old parameters. During the inference phase, when the Query-Key matching mechanism selects prompts for a specific task, the corresponding task’s adapter parameters will be loaded into the network’s adapter as well.

3.6. Loss Functions

Cosine Contrast Loss. We introduce a new contrast loss to ensure that the semantic prompts closely align with the features of class labels. Specifically, the class names will

be organized into the following form:

$$R_{sem,i} = \text{“A photo of } \{class\ i\} \text{.”} \quad (15)$$

to represent the class-level semantic expression for the i -th label in $Y(t)$. Next, they are encoded into semantic space $\xi_{sem,i} = \text{BERT}(R_{sem,i})$. Given the significant diversity in classes and domains within the dataset, we propose using a cosine-based function to enhance the stability of the learning process. The proposed cosine contrast loss is formulated as:

$$\mathcal{L}_{con} = \frac{1}{N_{inc}} \sum_{i=1}^{N_{inc}} \{ \hat{y}_i (1 - \cos(P_s, \xi_{sem,i})) + \alpha \cdot (1 - \hat{y}_i) |\cos(P_s, \xi_{sem,i})| \}, \quad (16)$$

where \hat{y}_i is a label indicating whether the sample pair is of the same class. $\hat{y}_i = 1$ indicates a positive sample pair, and $\hat{y}_i = 0$ indicates a negative sample pair.

In incremental tasks, the number of negative pairs often greatly exceeds that of positive pairs. For instance, in a 10-classes incremental stage, there is only one positive pair versus nine negative pairs. The imbalance makes it difficult for the model to learn from positive samples. To mitigate this issue, we introduce a trade-off factor α , empirically set to 0.3. By minimizing this *cosine contrast loss*, the model outputs P_s that are similar to their corresponding class-level semantic features. The adapter in the backbone network is thus guided to learn the correspondence between the semantic information and the image representation, thus improving the performance of image classification.

Classification Loss . In our approach, each task has its specific trainable classifier $\Phi(\cdot; \phi)$, which predicts the class of an image based on its features ξ_{cls} . Similar to previous methods, we use the cross entropy loss to optimize the classifier:

$$\mathcal{L}_{ce} = \text{CrossEntropy}(\Phi(\xi_{cls}; \phi), y). \quad (17)$$

Final Loss Function. In general, for task t , the final loss function combines the multi-key loss \mathcal{L}_k , cosine contrast loss \mathcal{L}_{con} , and CE loss \mathcal{L}_{ce} , forming the overall learning objective of the proposed model:

$$\mathcal{L} = \mathcal{L}_k + \mathcal{L}_{con} + \mathcal{L}_{ce}. \quad (18)$$

4. Experiments

4.1. Experimental Settings

Datasets. To compare with different continual learning methods, we conduct experiments on three benchmark datasets. Following the class-incremental learning setting [16, 32], task identities are not provided during testing.

- **ImageNetR** [17] is a dataset comprising 30,000 images across 200 classes derived from ImageNet. Each class

includes images in various styles, such as art, cartoons, graffiti, and challenging examples from the original ImageNet, introducing a significant domain shift. This diversity in styles makes the dataset particularly challenging for models trained on standard datasets.

- **CIFAR-100** [24] consists of 60,000 color images at a resolution of 32×32 pixels, categorized into 100 classes with 500 training images and 100 test images per class. It is a widely recognized benchmark in the continual learning community.
- **ImageNetA** [18] is a real-world dataset containing 7,500 unmodified, naturally occurring images from 200 ImageNet classes. These images were adversarially selected to be misclassified by ResNet models, presenting a substantial challenge for machine learning models. The dataset exhibits significant class imbalance, with some categories having very few samples.

Implementation Details. Following Cprompt [16], we employ the Stochastic Gradient Descent (SGD) optimizer [22] with a momentum of 0.9 and an initial learning rate of 0.01. Our experiments are conducted on an NVIDIA RTX 3090 GPU, with a batch size of 24 images per iteration. The learning rate decays to zero according to a cosine annealing schedule. We trained on ImageNetR for 14 epochs and trained 20 epochs on CIFAR100 and ImageNetA.

To evaluate our method in different incremental learning settings, we applied two strategies for ImageNetR and ImageNetA, each containing 200 classes. The first strategy splits the dataset into 10 tasks, with 20 classes per task, while the second divides it into 20 tasks, each containing 10 classes. For CIFAR100, which includes 100 classes, we partitioned it into 10 tasks, each containing 10 classes.

Evaluation Metrics. We evaluated our model using three widely adopted metrics in continual learning [16, 42, 47–49]. Specifically, we report the average prediction accuracy on all classes after the final training session, denoted as Last-acc, and the average accuracy across all sessions, denoted as Avg-acc. Additionally, we calculate the forgetting score FF, following the methodology in [42, 48], to quantify the performance degradation on previous tasks over time. To show the reliability and statistical significance of our results, we conducted each experiment three times using different random seeds to shuffle the dataset order. We report the mean performance metrics across these runs along with the corresponding standard deviations.

Compared Methods. To comprehensively demonstrate the superiority of our approach, we compare it against both prompt-based and adapter-based state-of-the-art (SOTA) continual learning methods. Specifically, the prompt-based methods we consider are L2P [49], DualPrompt [48], CODA-P [42], and CPrompt [16], while the adapter-based methods include EASE [55] and SSIAT [43]. These methods were chosen because they represent the current leading

Method	Split-ImageNetR			CIFAR100			Split-ImageNetA		
	Last-acc \uparrow	Avg-acc \uparrow	FF \downarrow	Last-acc \uparrow	Avg-acc \uparrow	FF \downarrow	Last-acc \uparrow	Avg-acc \uparrow	FF \downarrow
L2P[49]	69.11 \pm 0.42	75.61 \pm 0.80	7.93 \pm 0.05	82.44 \pm 0.56	88.00 \pm 0.97	7.04 \pm 1.48	44.29 \pm 0.74	53.93 \pm 1.05	9.98 \pm 0.15
DualPrompt[48]	71.50 \pm 0.23	76.62 \pm 0.68	6.03 \pm 0.88	83.07 \pm 0.55	88.41 \pm 1.19	6.22 \pm 1.43	46.65 \pm 0.19	58.06 \pm 0.91	12.69 \pm 1.11
CODA-P[42]	75.17 \pm 0.23	80.59 \pm 0.68	7.07 \pm 0.86	86.19 \pm 0.36	90.97 \pm 1.19	6.70 \pm 0.88	51.90 \pm 0.71	62.23 \pm 1.42	9.69 \pm 0.67
Cprompt[16]	76.93 \pm 0.55	82.45 \pm 0.80	<u>5.44</u> \pm 0.41	87.62 \pm 0.16	92.33 \pm 0.28	5.20 \pm 0.32	55.06 \pm 1.19	66.25 \pm 1.95	12.14 \pm 0.78
EASE[55]	76.16 \pm 0.25	82.85 \pm 0.46	7.45 \pm 0.34	88.12 \pm 0.56	92.49 \pm 0.75	5.83 \pm 0.60	54.16 \pm 0.20	65.98 \pm 0.78	13.05 \pm 0.82
SSIAT[43]	79.90 \pm 0.43	84.06 \pm 0.64	5.91 \pm 0.43	<u>91.43</u> \pm 0.16	<u>94.27</u> \pm 0.74	<u>4.63</u> \pm 0.48	<u>61.29</u> \pm 1.10	<u>69.91</u> \pm 1.54	15.67 \pm 0.68
AESP(ours)	81.95 \pm 0.50	86.06 \pm 0.48	4.53 \pm 0.22	92.69 \pm 0.19	95.19 \pm 0.07	2.87 \pm 0.27	63.99 \pm 0.68	72.01 \pm 0.78	10.08 \pm 0.10

Table 1. Comparison of performance on Split-ImageNetR, CIFAR100, and Split-ImageNetA under the 10-task setting. The first four rows display the prompt-based methods, the following two rows present the adapter-based methods, and the proposed AESP is shown in the last row. The best result is marked in **bold**, and the second-best result is underlined.

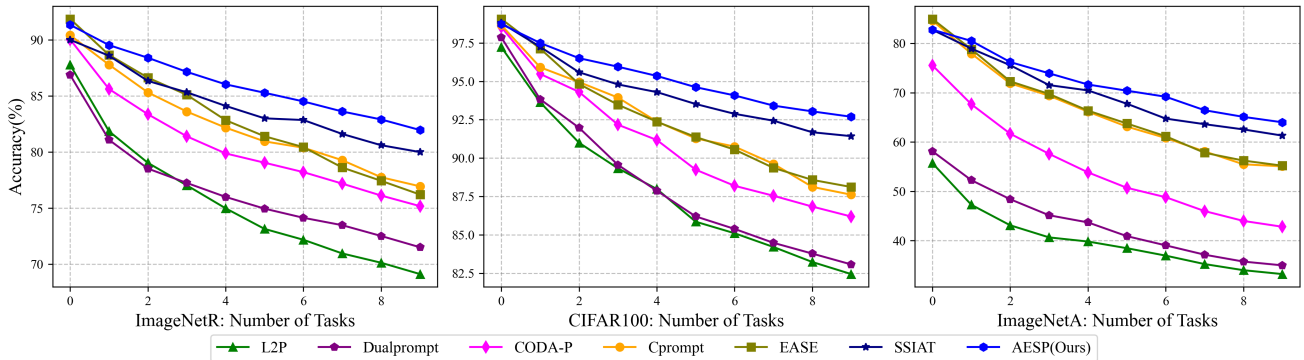


Figure 3. Illustrations of the continual learning performance at each task are depicted through these curves. The curves are constructed by averaging the performance across three separate seeds for every incremental learning session.

Method	Split-ImageNetR		Split-ImageNetA	
	Last-acc \uparrow	Avg-acc \uparrow	Last-acc \uparrow	Avg-acc \uparrow
L2P[49]	65.88 \pm 0.33	73.18 \pm 1.37	37.16 \pm 0.36	47.95 \pm 0.43
Dual-P[48]	67.80 \pm 0.51	73.82 \pm 1.45	39.76 \pm 0.24	53.67 \pm 0.72
CODA-P[42]	72.41 \pm 0.37	77.98 \pm 1.01	43.78 \pm 0.57	56.03 \pm 0.69
Cprompt[16]	74.31 \pm 0.79	81.18 \pm 0.15	52.29 \pm 0.81	64.02 \pm 1.26
EASE[55]	74.09 \pm 0.36	81.51 \pm 0.47	42.42 \pm 1.29	57.36 \pm 1.26
SSIAT[43]	<u>78.32</u> \pm 0.36	<u>82.99</u> \pm 0.68	<u>58.45</u> \pm 2.23	<u>68.03</u> \pm 2.18
AESP(ours)	79.75 \pm 0.52	84.48 \pm 0.53	60.96 \pm 0.76	70.28 \pm 0.98

Table 2. Experimental results under 20-task setting on Split-ImageNetR and Split-ImageNetA dataset. The best result is marked in **bold**, and the second-best result is underlined.

techniques in their respective categories, providing a robust benchmark for evaluation. For a fair comparison, we reproduce the best results of these methods under the same experimental environments. Additionally, all results are averaged over three runs with different random seeds to ensure statistical reliability.

4.2. Main Results

As shown in Table 1, the proposed AESP method outperformed across all datasets when compared to SOTA methods. First, we report the experimental results on the ImageNetR and CIFAR100 datasets. Our method demon-

strates a substantial improvement over prompt-based approaches. Notably, although Cprompt has achieved significant advancements over earlier prompt-based methods, our approach surpasses it on ImageNetR by 5.02% in Last-acc, 3.61% in Avg-acc, and 1.38% lower than it in forgetting rate. Similarly, on CIFAR100, AESP exceeds Cprompt by 4.87% in Last-acc and 2.66% in Avg-acc. In terms of forgetfulness, it’s almost 2% lower.

Moreover, while the latest adapter-based methods have previously outperformed prompt-based methods, our AESP method which integrates both adapters and prompts, successfully surpasses these adapter-based approaches. Specifically, we achieve improvements of 2.05% in Last-acc and 2% in Avg-acc on ImageNetR over the best-performing adapter-based method SSIAT. While our lead in Last-acc over prompt-based methods is notable, our advantage in Avg-acc over adapter-based methods is even more pronounced. This is because adapter-based methods tend to exhibit stronger resistance to catastrophic forgetting. By combining adapters with prompts, our approach effectively inherits this strength, reducing the forgetting rate by approximately 1.38% compared to SSIAT on ImageNetR and 1.76% on CIFAR100.

ImageNetA is a particularly challenging dataset, as it comprises samples that are frequently misclassified by

Method	Split-ImageNetR			CIFAR100			Split-ImageNetA		
	Last-acc \uparrow	Avg-acc \uparrow	FF \downarrow	Last-acc \uparrow	Avg-acc \uparrow	FF \downarrow	Last-acc \uparrow	Avg-acc \uparrow	FF \downarrow
w/o Adapter	80.29	84.53	4.43	91.31	94.14	3.15	62.78	68.36	8.58
w/o S-Prompt	79.99	84.26	4.58	91.23	94.18	3.21	64.12	71.36	9.71
w/o IQKM	74.39	80.74	8.25	84.54	90.06	6.81	53.87	64.59	16.17
AESP	81.95	86.06	4.53	92.69	95.19	2.87	63.99	72.01	10.08

Table 3. Ablation Study on Split-ImageNetR, CIFAR100, and Split-ImageNetA dataset. We removed the Adapter, Semantic Prompt (S-Prompt), and Integrated query-key matching (IQKM) from the model separately to verify the validity of each component.

Attach Layer	Amount	Last-acc \uparrow	Avg-acc \uparrow
Layer 0 - 3	4	81.08	85.15
Layer 8 - 11	4	80.10	84.25
Layer 0 - 4	5	81.16	85.11
Layer 7 - 11	5	80.98	84.83
Layer 0 - 5	6	81.33	85.55
Layer 6 - 11	6	81.12	85.40
Layer 0 - 11	12	81.95	86.06

Table 4. The influence of Adapters for different layers. Experiments were performed on the Split-imagenetR dataset.

ResNet models due to their adversarial or anomalous nature. However, our proposed method leverages the strong generalization capabilities of semantic information, enhancing image feature representations and thereby improving the classification accuracy of these difficult samples. Our method achieves Last-acc and Avg-acc of 63.99% and 72.01%, respectively, representing improvements of about 1.56% and 1.18% over SSIAT. A detailed comparison of the different continual learning methods in the three datasets is shown in Figure 3.

Additionally, we evaluate our method under a 20-task setting to assess its performance in scenarios involving long sequences of tasks. As shown in Table 2. Under the 20-task setting, our method achieves a Last-acc of 79.75% on ImageNetR and 60.96% on ImageNetA, maintaining leading performance. These results are 1.43% higher than SSIAT and ahead of Cprompt by as much as 5.44%. A similar trend is observed for Avg-acc, indicating that our method maintains good stability and strong resistance to forgetting when dealing with longer task sequences.

4.3. Ablation Study

We conducted ablation experiments under the 10-task setting on three datasets to evaluate the effectiveness of three components: adapters, semantic prompts, and integrated query-key matching (IQKM). The results are shown in Table 3. First, when we removed the adapter from the ViT layers, the Last-acc dropped by 1.66%, 1.38%, and 1.21% on ImageNetR, CIFAR100, and ImageNetA, respectively, while the Avg-acc decreased by 1.53%, 1.05%, and 3.65%. This consistent decline across all datasets indicates that in-

tegrating the adapter is crucial for learning adaptive features.

Next, removing the semantic prompts resulted in a decrease in Last-acc by 1.96% on ImageNetR and 1.46% on CIFAR100. Interestingly, on ImageNetA, the Last-acc slightly increased by 0.13%. The Avg-acc dropped by 1.80%, 1.01%, and 0.65% on the three datasets, respectively. These results suggest that while semantic prompts generally assist in feature adaptation and lead to more generalized feature representations, their impact may vary depending on the dataset characteristics.

Finally, replacing the IQKM module with the Multi-Key mechanism from CPrompt [16] for query-key matching led to significant performance drops across all datasets. The Last-acc decreased by 7.56%, 8.15%, and 10.12% on the three datasets respectively, and the Avg-acc fell by 5.32%, 5.13%, and 7.42%. This substantial decline aligns with our expectations: inaccurate task selection can cause the adapter and prompt to provide incorrect prompts and semantic guidance, conflicting with the model’s pre-trained knowledge and leading to suboptimal results.

Impact of adapter location. Layers at different depths of ViT exhibit varying feature extraction capabilities. On the ImageNetR dataset, we explored the impact of fine-tuning ViT layers at different depths under the 10-task setting on model performance. Table 4 reports the results of adding adapters at different depths.

It is clear that incorporating adapters in all layers of the ViT remains the most effective approach. Additionally, attaching adapters to shallow layers yields better results than to deep layers. This phenomenon differs somewhat from previous findings [15, 35]. Earlier adapter-based methods primarily handled pure image information, whereas our method integrates semantic information, requiring adapters to align both semantic and image features at varying depths. This shows to some extent that our approach optimizes the model’s internal learning process and feature extraction capabilities.

5. Conclusion

In this paper, we design a novel adapter-enhanced semantic prompting framework for continual learning, which

combines the benefits of prompts and adapters. To enhance the generalization ability of visual features, we introduce semantic prompts generated by the large language model BERT and design a cosine contrast loss for effective learning. Furthermore, we propose an integrated query-key matching mechanism to improve the accuracy of task prompt selection, which facilitates final image classification. Extensive experiments on three widely used continual learning datasets demonstrate the effectiveness of our proposed framework.

References

- [1] Hongjoon Ahn, Sungmin Cha, Donggyu Lee, and Taesup Moon. Uncertainty-based continual learning with adaptive regularization. In *NeurIPS*, pages 4394–4404, 2019. 2
- [2] Rahaf Aljundi, Francesca Babiloni, Mohamed Elhoseiny, Marcus Rohrbach, and Tinne Tuytelaars. Memory aware synapses: Learning what (not) to forget. In *ECCV*, pages 144–161, 2018. 1
- [3] Jihwan Bang, Heesu Kim, Youngjoon Yoo, Jung-Woo Ha, and Jonghyun Choi. Rainbow memory: Continual learning with a memory of diverse samples. In *CVPR*, pages 8218–8227, 2021. 1, 2
- [4] Eden Belouadah, Adrian Popescu, and Ioannis Kanellos. A comprehensive study of class incremental learning algorithms for visual tasks. *Neural Networks*, 135:38–54, 2021. 1, 2
- [5] Chen Bojian, Shen Changqing, Shi Juanjuan, Kong Lin, Tan Luyang, Wang Dong, and Zhu Zhongkui. Continual learning fault diagnosis: A dual-branch adaptive aggregation residual network for fault diagnosis with machine increments. *Chinese Journal of Aeronautics*, 36(6):361–377, 2023. 1
- [6] Lorenzo Bonicelli, Matteo Boschini, Angelo Porrello, Conetto Spampinato, and Simone Calderara. On the effectiveness of lipschitz-driven rehearsal in continual learning. In *NeurIPS*, 2022. 2
- [7] Leo Breiman. Random forests. *Mach. Learn.*, 45(1):5–32, 2001. 5
- [8] Hanting Chen, Yunhe Wang, Tianyu Guo, Chang Xu, Yiping Deng, Zhenhua Liu, Siwei Ma, Chunjing Xu, Chao Xu, and Wen Gao. Pre-trained image processing transformer. In *CVPR*, pages 12299–12310, 2021. 2
- [9] Shoufa Chen, Chongjian Ge, Zhan Tong, Jiangliu Wang, Yibing Song, Jue Wang, and Ping Luo. Adaptformer: Adapting vision transformers for scalable visual recognition. In *NeurIPS*, 2022. 3
- [10] Jacob Devlin, Ming-Wei Chang, Kenton Lee, and Kristina Toutanova. BERT: pre-training of deep bidirectional transformers for language understanding. In *NAACL-HLT*, pages 4171–4186, 2019. 1, 4
- [11] Songlin Dong, Xiaopeng Hong, Xiaoyu Tao, Xinyuan Chang, Xing Wei, and Yihong Gong. Few-shot class-incremental learning via relation knowledge distillation. In *AAAI*, pages 1255–1263, 2021. 2
- [12] Alexey Dosovitskiy, Lucas Beyer, Alexander Kolesnikov, Dirk Weissenborn, Xiaohua Zhai, Thomas Unterthiner, Mostafa Dehghani, Matthias Minderer, Georg Heigold, Sylvain Gelly, Jakob Uszkoreit, and Neil Houlsby. An image is worth 16x16 words: Transformers for image recognition at scale. In *ICLR*, 2021. 4
- [13] Robert M French. Catastrophic forgetting in connectionist networks. *Trends in Cognitive Sciences*, 3(4):128–135, 1999. 1, 2
- [14] Xinyuan Gao, Yuhang He, Songlin Dong, Jie Cheng, Xing Wei, and Yihong Gong. DKT: diverse knowledge transfer transformer for class incremental learning. In *CVPR*, pages 24236–24245, 2023. 2, 4
- [15] Xinyuan Gao, Songlin Dong, Yuhang He, Qiang Wang, and Yihong Gong. Beyond prompt learning: Continual adapter for efficient rehearsal-free continual learning. *arXiv preprint arXiv:2407.10281*, 2024. 1, 3, 8
- [16] Zhanxin Gao, Jun Cen, and Xiaobin Chang. Consistent prompting for rehearsal-free continual learning. In *CVPR*, pages 28463–28473, 2024. 3, 4, 6, 7, 8
- [17] Dan Hendrycks, Steven Basart, Norman Mu, Saurav Kadavath, Frank Wang, Evan Dorundo, Rahul Desai, Tyler Zhu, Samyak Parajuli, Mike Guo, Dawn Song, Jacob Steinhardt, and Justin Gilmer. The many faces of robustness: A critical analysis of out-of-distribution generalization. In *CVPR*, pages 8320–8329, 2021. 6
- [18] Dan Hendrycks, Kevin Zhao, Steven Basart, Jacob Steinhardt, and Dawn Song. Natural adversarial examples. In *CVPR*, pages 15262–15271, 2021. 6
- [19] Saihui Hou, Xinyu Pan, Chen Change Loy, Zilei Wang, and Dahua Lin. Learning a unified classifier incrementally via rebalancing. In *CVPR*, pages 831–839, 2019. 1
- [20] Neil Houlsby, Andrei Giurgiu, Stanislaw Jastrzebski, Bruna Morrone, Quentin de Laroussilhe, Andrea Gesmundo, Mona Attariyan, and Sylvain Gelly. Parameter-efficient transfer learning for NLP. In *ICML*, pages 2790–2799, 2019. 3
- [21] Michael I Jordan and Tom M Mitchell. Machine learning: Trends, perspectives, and prospects. *Science*, 349(6245):255–260, 2015. 1
- [22] Nitish Shirish Keskar and Richard Socher. Improving generalization performance by switching from adam to sgd. *arXiv preprint arXiv:1712.07628*, 2017. 6
- [23] Muhammad Gul Zain Ali Khan, Muhammad Ferjad Naeem, Luc Van Gool, Didier Stricker, Federico Tombari, and Muhammad Zeshan Afzal. Introducing language guidance in prompt-based continual learning. In *ICCV*, pages 11429–11439, 2023. 1
- [24] Alex Krizhevsky and Geoffrey Hinton. Learning multiple layers of features from tiny images. Technical report, University of Toronto, 2009. 6
- [25] Matthias De Lange, Rahaf Aljundi, Marc Masana, Sarah Parisot, Xu Jia, Ales Leonardis, Gregory G. Slabaugh, and Tinne Tuytelaars. A continual learning survey: Defying forgetting in classification tasks. *IEEE TPAMI*, 44(7):3366–3385, 2022. 1, 2
- [26] Jin Li, Zhong Ji, Gang Wang, Qiang Wang, and Feng Gao. Learning from students: Online contrastive distillation network for general continual learning. In *IJCAI*, pages 3215–3221, 2022. 2

- [27] Xiaorong Li, Shipeng Wang, Jian Sun, and Zongben Xu. Variational data-free knowledge distillation for continual learning. *IEEE TPAMI*, 45(10):12618–12634, 2023. 2
- [28] Pengfei Liu, Weizhe Yuan, Jinlan Fu, Zhengbao Jiang, Hiroaki Hayashi, and Graham Neubig. Pre-train, prompt, and predict: A systematic survey of prompting methods in natural language processing. *ACM Comput. Surv.*, 55(9):195:1–195:35, 2023. 2
- [29] David Lopez-Paz and Marc’Aurelio Ranzato. Gradient episodic memory for continual learning. In *NeurIPS*, 2017. 1
- [30] Batta Mahesh. Machine learning algorithms-a review. *International Journal of Science and Research.*, 9(1):381–386, 2020. 1
- [31] Michael McCloskey and Neal J Cohen. Catastrophic interference in connectionist networks: The sequential learning problem. In *Psychology of Learning and Motivation*, pages 109–165, 1989. 1, 2
- [32] Sudhanshu Mittal, Silvio Galesso, and Thomas Brox. Essentials for class incremental learning. In *CVPRW*, pages 3513–3522, 2021. 4, 6
- [33] Ismoilov Nusrat and Sung-Bong Jang. A comparison of regularization techniques in deep neural networks. *Symmetry*, 10(11):648, 2018. 2
- [34] German I Parisi, Ronald Kemker, Jose L Part, Christopher Kanan, and Stefan Wermter. Continual lifelong learning with neural networks: A review. *Neural networks*, 113:54–71, 2019. 1
- [35] Keon-Hee Park, Kyungwoo Song, and Gyeong-Moon Park. Pre-trained vision and language transformers are few-shot incremental learners. In *CVPR*, pages 23881–23890, 2024. 1, 8
- [36] Wenjie Pei, Tongqi Xia, Fanglin Chen, Jinsong Li, Jiandong Tian, and Guangming Lu. Sa²vp: Spatially aligned-and-adapted visual prompt. In *AAAI*, pages 4450–4458, 2024. 2
- [37] Farhad Pourpanah, Moloud Abdar, Yuxuan Luo, Xinlei Zhou, Ran Wang, Chee Peng Lim, Xi-Zhao Wang, and Q. M. Jonathan Wu. A review of generalized zero-shot learning methods. *IEEE TPAMI*, 45(4):4051–4070, 2023. 2
- [38] Alec Radford, Jong Wook Kim, Chris Hallacy, Aditya Ramesh, Gabriel Goh, Sandhini Agarwal, Girish Sastry, Amanda Askell, Pamela Mishkin, Jack Clark, Gretchen Krueger, and Ilya Sutskever. Learning transferable visual models from natural language supervision. In *ICML*, pages 8748–8763, 2021. 1
- [39] Mengye Ren, Renjie Liao, Ethan Fetaya, and Richard Zemel. Incremental few-shot learning with attention attractor networks. In *NeurIPS*, 2019. 1
- [40] Jonathan Schwarz, Wojciech Czarnecki, Jelena Luketina, Agnieszka Grabska-Barwinska, Yee Whye Teh, Razvan Pascanu, and Raia Hadsell. Progress & compress: A scalable framework for continual learning. In *ICML*, pages 4535–4544, 2018. 2
- [41] Guangyuan Shi, Jiaxin Chen, Wenlong Zhang, Li-Ming Zhan, and Xiao-Ming Wu. Overcoming catastrophic forgetting in incremental few-shot learning by finding flat minima. In *NeurIPS*, pages 6747–6761, 2021. 1, 2
- [42] James Seale Smith, Leonid Karlinsky, Vyshnavi Gutta, Paola Cascante-Bonilla, Donghyun Kim, Assaf Arbelle, Rameswar Panda, Rogério Feris, and Zsolt Kira. Coda-prompt: Continual decomposed attention-based prompting for rehearsal-free continual learning. In *CVPR*, pages 11909–11919, 2023. 3, 6, 7
- [43] Yuwen Tan, Qin hao Zhou, Xiang Xiang, Ke Wang, Yuchuan Wu, and Yongbin Li. Semantically-shifted incremental adapter-tuning is A continual vitransformer. In *CVPR*, pages 23252–23262, 2024. 3, 6, 7
- [44] Yu-Ming Tang, Yi-Xing Peng, and Wei-Shi Zheng. When prompt-based incremental learning does not meet strong pre-training. In *ICCV*, pages 1706–1716, 2023. 1
- [45] Xiaoyu Tao, Xinyuan Chang, Xiaopeng Hong, Xing Wei, and Yihong Gong. Topology-preserving class-incremental learning. In *ECCV*, pages 254–270, 2020. 1
- [46] Songsong Tian, Lusi Li, Weijun Li, Hang Ran, Xin Ning, and Prayag Tiwari. A survey on few-shot class-incremental learning. *Neural Networks*, 169:307–324, 2024. 1
- [47] Liyuan Wang, Xingxing Zhang, Hang Su, and Jun Zhu. A comprehensive survey of continual learning: Theory, method and application. *IEEE TPAMI*, 46(8):5362–5383, 2024. 1, 2, 6
- [48] Zifeng Wang, Zizhao Zhang, Sayna Ebrahimi, Ruoxi Sun, Han Zhang, Chen-Yu Lee, Xiaoqi Ren, Guolong Su, Vincent Perot, Jennifer G. Dy, and Tomas Pfister. Dualprompt: Complementary prompting for rehearsal-free continual learning. In *ECCV*, pages 631–648, 2022. 1, 3, 5, 6, 7
- [49] Zifeng Wang, Zizhao Zhang, Chen-Yu Lee, Han Zhang, Ruoxi Sun, Xiaoqi Ren, Guolong Su, Vincent Perot, Jennifer G. Dy, and Tomas Pfister. Learning to prompt for continual learning. In *CVPR*, pages 139–149, 2022. 1, 3, 5, 6, 7
- [50] Jie Zhang, Juntao Zhang, Shalini Ghosh, Dawei Li, Jingwen Zhu, Heming Zhang, and Yalin Wang. Regularize, expand and compress: Nonexpansive continual learning. In *WACV*, pages 843–851, 2020. 2
- [51] Peiyan Zhang, Yuchen Yan, Chaozhuo Li, Senzhang Wang, Xing Xie, Guojie Song, and Sunghun Kim. Continual learning on dynamic graphs via parameter isolation. In *ACM SIGIR*, pages 601–611, 2023. 2
- [52] Zhilu Zhang and Mert R. Sabuncu. Generalized cross entropy loss for training deep neural networks with noisy labels. In *NeurIPS*, pages 8792–8802, 2018. 5
- [53] Haiyan Zhao, Tianyi Zhou, Guodong Long, Jing Jiang, and Chengqi Zhang. Does continual learning equally forget all parameters? In *ICML*, pages 42280–42303, 2023. 2
- [54] Da-Wei Zhou, Yuanhan Zhang, Jingyi Ning, Han-Jia Ye, De-Chuan Zhan, and Ziwei Liu. Learning without forgetting for vision-language models. *arXiv preprint arXiv:2305.19270*, 2023. 2
- [55] Da-Wei Zhou, Hai-Long Sun, Han-Jia Ye, and De-Chuan Zhan. Expandable subspace ensemble for pre-trained model-based class-incremental learning. In *CVPR*, pages 23554–23564, 2024. 3, 6, 7
- [56] Da-Wei Zhou, Qi-Wei Wang, Zhi-Hong Qi, Han-Jia Ye, De-Chuan Zhan, and Ziwei Liu. Class-incremental learning: A survey. In *IEEE TPAMI*, 2024. 1, 2, 4